



Densities and volumes of hydrous silicate melts: New measurements and predictions

Mohamed Ali M.A. Bouhifd, A.G. Whittington, Pascal Richet

► To cite this version:

Mohamed Ali M.A. Bouhifd, A.G. Whittington, Pascal Richet. Densities and volumes of hydrous silicate melts: New measurements and predictions. *Chemical Geology*, 2015, 418, pp.40-50. 10.1016/j.chemgeo.2015.01.012 . insu-01443455

HAL Id: insu-01443455

<https://insu.hal.science/insu-01443455>

Submitted on 6 Aug 2020

HAL is a multi-disciplinary open access archive for the deposit and dissemination of scientific research documents, whether they are published or not. The documents may come from teaching and research institutions in France or abroad, or from public or private research centers.

L'archive ouverte pluridisciplinaire **HAL**, est destinée au dépôt et à la diffusion de documents scientifiques de niveau recherche, publiés ou non, émanant des établissements d'enseignement et de recherche français ou étrangers, des laboratoires publics ou privés.

Densities and Volumes of Hydrous Silicate Melts:

New Measurements and Predictions

M.A. Bouhifd¹, A.G. Whittington² and P. Richet³

¹Laboratoire Magmas et Volcans, CNRS UMR 6524, Université Blaise Pascal, OPGC-IRD,
5 Rue Kessler, 63038 Clermont-Ferrand Cedex, France

²Department of Geological Sciences, 101 Geology Building, University of Missouri,
Columbia, MO 65211, USA

³Institut de Physique du Globe de Paris, 1 Rue Jussieu, 75005 Paris, France

Abstract

The equilibrium molar volumes of four series of anhydrous and hydrous aluminosilicate glasses and liquids (0 to 11 mol% H₂O) were determined at one bar between 300 and 1050 K. The anhydrous compositions range from highly polymerized NaAlSi₃O₈ to depolymerized synthetic iron-free analogues of tephrite and foidite magma compositions (NBO/T = 0.8 and 1.5, respectively). For each sample the volume was derived from the room-temperature density of the glass and the thermal expansivity of the glass and supercooled liquid from 300 K to a temperature about 50 K higher than the standard glass transition. The partial molar coefficient of thermal expansion of water in hydrous silicate glasses is about $(6.2 \pm 3.5) \times 10^{-5}$ K⁻¹, and in the melts ranges from 11×10^{-5} to 36×10^{-5} K⁻¹. The present molar volumes of hydrous supercooled liquids are reproduced with the model of Ochs and Lange (1999) to within 1.1%, except for the hydrous foidite series. This agreement confirms that the partial molar volume of water ($\bar{V}_{\text{H}_2\text{O}}$) near the glass transition cannot depend strongly on the chemical composition of the silicate end-member, nor on water speciation. In order to reproduce the molar volumes of the foidite series, a combined model (using Lange (1997) and Courtial and Dingwell (1999) models and values derived from the new data) is used where an excess volume term between SiO₂ and CaO is introduced. Finally, our experimental data are better fit if $\bar{V}_{\text{H}_2\text{O}} = 23.8 \pm 0.5$ cm³ mol⁻¹ at 1273 K, and $\frac{d\bar{V}_{\text{H}_2\text{O}}}{dT} = 15.9 \pm 1.5$ cm³ mol⁻¹ K⁻¹. Contrasting trends are also observed for the configurational contributions to the expansivity

- 32 with a positive slope of $\frac{dV_i^{conf}}{dT}$ versus water for the most polymerized base compositions
33 ($NBO/T \leq 0.21$) and a negative slope for the two most depolymerized base compositions with
34 NBO/T of 0.86 and 1.51.

1. Introduction

As a major component of magmatic melts, water owes its importance to the influence it exerts on their physical and chemical properties, and hence on magma ascent and phase equilibria. The density of silicate liquids is for instance a critical parameter to determine the depth at which crystal-melt density inversions occur (Agee, 2008). Water has recently been suggested to play a critical role in buoyancy triggered supervolcano eruptions (Malfait et al., 2014a). Its exceptional effects on viscosity are now rather well documented: for example, addition of 1000 ppm H₂O lowers the viscosity of pure SiO₂ by 10 orders of magnitude in the glass transition range (*e.g.* Mysen and Richet, 2005; and references therein). Even though effects on density are usually less extreme, water nonetheless remains an important component due to its low molecular weight, so that a 5 wt% water content translates into about 15 mol % on an oxide basis. The effect of dissolved water on volume properties is thus necessarily significant (Burnham and Davis, 1971).

Following Bottinga and Weill (1970), various authors have empirically set predictive models of partial molar volumes (\bar{V}_i) and expansivities ($\partial\bar{V}_i/\partial T$) of oxide components over wide temperature and composition ranges (*e.g.*, Bottinga et al., 1982; Knoche et al., 1995; Lange and Carmichael, 1987; Lange, 1997). For hydrous silicate glasses, a review of available density data indicated that the room-temperature partial molar volume of H₂O ($\bar{V}_{\text{H}_2\text{O}}$) is independent of glass composition with a value of 12.0±0.5 cm³ mol⁻¹ (Richet et al., 2000). This value is thus valid for polymerized, silica-rich to depolymerized, silica-poor composition at 1 bar, but the partial molar compressibility of water markedly depends on composition, indicating that $\bar{V}_{\text{H}_2\text{O}}$ may depend on melt composition at high pressure (Malfait et al., 2011; Whittington et al., 2012). In fact, a compositionally dependent $\bar{V}_{\text{H}_2\text{O}}$ at high pressure has also been suggested based on the pressure dependence of water solubility in silicate melts (Mysen and Acton, 1999; Mysen and Wheeler, 2000). For

instance the latter authors calculated a $\bar{V}_{\text{H}_2\text{O}}$ in haploandesitic melts from solubility data which was negatively correlated with Al_2O_3 content. Despite these indications Malfait et al. (2014b) have shown that, within the experimental uncertainties of about 1.3%, the $\bar{V}_{\text{H}_2\text{O}}$ is independent of the silicate melt composition.

Few volume measurements exist for hydrous silicate melts at atmospheric pressure (*e.g.* Burnham and Davis, 1971; Ochs and Lange, 1997; 1999; Bouhifd et al., 2001). From their own expansivity measurements for three samples and the high-temperature, high-pressure measurements of Burnham and Davis (1971) for a hydrous albite liquid, Ochs and Lange (1997, 1999) reported that dissolved water has a $\bar{V}_{\text{H}_2\text{O}} = 22.9 \pm 0.6 \text{ cm}^3 \text{ mol}^{-1}$ at 1273 K and 1 bar.

The main aim of the present study was to expand the available database for the 1-bar density and volume of hydrous silicate glasses and liquids at high temperatures, knowing that derivation of the pressure dependence of silicate liquid volumes depends upon accurate 1 bar values as a function of temperature. Another aim of this work was to determine whether the results for $\bar{V}_{\text{H}_2\text{O}}$ previously obtained are applicable to a composition range wider than that of their input data.

We have thus measured the thermal expansion of hydrous glasses and liquids of four synthetic iron-free series modeled after albite, tephrite, trachyte, and basanite/foidite (hereafter “foidite” with individual samples labeled “NIQ”) whose compositions are reported in Table 1. Also included in Table 1 is the sample selected in our preliminary study to derive the partial molar volume of water in phonolitic glasses and liquids (Bouhifd et al., 2001). The whole set of samples represent the range of polymerization states relevant to natural magmas, and has been the subject of previous investigations of heat capacity (Bouhifd et al., 2006; 2013), viscosity (Whittington et al., 2000; 2001; 2004; 2009), and compressibility (Richet et al., 2000; Whittington et al., 2012).

85

86 **2. Experimental methods**

87 The anhydrous glasses were synthesized from oxide and carbonate mixes through
88 repeated cycles of grinding and fusion at about 1600 °C. The chemical compositions are
89 reported in Table 1 as analyzed with the electron microprobe. The samples were then
90 hydrated at high temperatures at either 2 or 3 kbar in an internally heated vessel with the
91 procedure reported by Whittington et al. (2000). The hydration conditions and the water
92 contents measured by Karl-Fischer titration are given in Table 2. Samples of about 10 mg
93 were analyzed in this study, for which the uncertainty on the reported water content is
94 around 0.1 wt% H₂O (Behrens et al., 1996). The room-temperature densities of the glasses
95 included in Table 3 were measured by an Archimedean method with toluene as the
96 immersion liquid.

97 Because the samples were initially densified as a result of their high-pressure
98 synthesis, the density of the sample was again measured after each thermal expansion
99 measurement to determine the extent of possible volume relaxation. Likewise, we checked
100 by weighing that no water loss occurred on heating at the highest temperatures. For the
101 hydrous glasses, the densities of the initial and relaxed glasses after expansivity
102 measurements are listed in Table 3.

103 The dilatometry apparatus was described in detail by Sipp and Richet (2002). Briefly,
104 the furnace was made of two Fibrothal half shells (from Kanthal) and regulated with a
105 P.I.D. controller. Temperatures were measured with a Pt-Pt/Rh 10% thermocouple placed
106 next to the sample. Upon heating we measured the length of the sample as a function of
107 temperature as the difference between the displacement of two SiO₂ rods, one resting on
108 the sample and the other on a reference cylinder of SiO₂ glass. These measurements were
109 made to within about 0.2 μm with linear variable differential transducers. Silica was

chosen as a reference material because its expansivity is approximately zero over the studied temperature intervals.

Because glasses and liquids are isotropic, the volume coefficient of thermal expansion α of all samples was obtained simply by multiplying the linear coefficient α_{linear} by 3:

$$\alpha_{\text{glass or liquid}} = 3 \times \alpha_{\text{linear}} = 3/L \left(\partial L / \partial T \right) = 3 \times \partial \ln(L) / \partial T \quad (1)$$

where L is the length of the sample and T its temperature. To determine the coefficients of thermal expansion of glasses and liquids we have adopted the procedure described by Toplis and Richet (2000) for anhydrous silicate melts. Contrasting with the usual method with which samples are continuously heated through the glass transition, this procedure ensures that measurements are made for supercooled silicate liquids that are in internal thermodynamic equilibrium. The resulting improvement is that thermal expansion coefficients can then be derived in a rigorous way from the sample length measured. At the beginning of the experiments the samples were heated continuously at a constant rate of 2 K min⁻¹ from room temperature to a temperature corresponding to a viscosity of 10¹³ Pa s (T_{13}), known from our previous viscosity experiments. For liquids, this T_{13} was then taken as a reference temperature at which the sample was first held until a constant length was observed. The temperature of the sample was then increased or decreased by 10 K steps at 2 K min⁻¹ and kept constant until a new equilibrium length was reached. Different temperatures over a range of ~50 to 70 degrees were studied in this manner. The time spent at each temperature was variable, more time being required at lower temperatures because of slower relaxation kinetics.

An important feature of this protocol is that two or more length changes can be measured for each temperature (i.e., upon heating and cooling), providing checks that the measured lengths do represent equilibrium values. This is the procedure described by Toplis and Richet (2000) for anhydrous samples, with the exception that we did not make a

final measurement at T_{13} , to limit the duration of the experiment and thus reduce the risk of water exsolution. The slowness of water exsolution in the temperature interval investigated makes accurate measurements possible in the supercooled liquid state near the glass transition. Because length changes are measured with high precision, the expansivities are generally determined to better than 3% (Toplis and Richet 2000). In this work we have set a conservative upper limit of 5% for the experimental uncertainty.

3. Results

All experimental data for the thermal expansion of anhydrous and hydrous glasses and liquids are reported in Tables 4-5.

Thermal expansion of hydrous glasses

In the initial measurements made on unrelaxed samples, expansion began to be anomalously high at temperatures at which the viscosity was about 10^{16} Pa s as indicated by extrapolation of the viscosity measurements by Whittington et al. (2000; 2001; 2004). This anomaly signaled the onset of volume relaxation to the 1-bar density of the samples, which were initially compacted as a result of their high pressure synthesis (Fig. 1). A second measurement was then performed with the same heating rate on the relaxed sample during which the sample length increased linearly with temperature up to T_{13} . No variations of mass or room-temperature density were observed after this second measurement.

For each glass we calculated the thermal expansion coefficient between room temperature and the highest temperature up to which expansion was linear, *i.e.*, up to the onset of volume relaxation for densified glasses and up to about T_{13} for relaxed glasses. The calculated thermal expansion coefficients of densified glasses are systematically

higher than those of relaxed glasses by about 3 - 6 %, except for the sample “Teph 0.3” for which a reverse effect is observed (*cf.* Table 5). These contrasts demonstrate that differences in fictive pressures of only 2 or 3 kbar have minor but detectable effects on glass expansivity.

Thermal expansion of hydrous liquids

The experiments were made on liquids over temperature intervals of up to 70 degrees (*cf.* Fig. 2 a-d). Because the glass transition is lowered with increasing water contents, so were the temperatures ranges investigated. Although minor penetration of the SiO₂ rod into the sample took place at the highest temperatures, this effect was readily taken into account with the procedure described by Toplis and Richet (2000) to determine the equilibrium length. Within experimental uncertainties, the logarithm of the length varied linearly with temperature for all supercooled liquids (see Fig. 2 for the hydrous Tephrite series). The slopes of these lines thus represent the linear thermal expansion coefficient, which could thus be determined from equation (1) and clearly increases with increasing water contents.

Possible water loss was a serious concern because the water contents of the samples were much higher than the 1-bar solubility of water. However, no changes in sample weight were observed after the experiments. As a more sensitive check, the viscosity of the same supercooled liquids was measured in the same temperature ranges. No influence of thermal history on the measured viscosities was apparent and the variations of the viscosities with temperature were as smooth as for water-free samples. Owing to the tremendous influence of water on viscosity, this excellent precision demonstrates unequivocally, as discussed by Whittington et al. (2004), the lack of detectable water loss during high-temperature measurements as long as the viscosity was higher than about 10⁹ Pa.s. Similar observations were made in viscosity measurements on andesite samples

which had the same room-temperature infrared spectra prior to and after high-temperature viscometry (Richet et al., 1996).

Volume of dry and hydrous silicate glasses

From 300 K to the glass transition, the volume of each glass sample was calculated from:

$$V_{\text{glass}}(T) = V_{\text{glass}}(300 \text{ K}) \exp(\alpha_{\text{glass}}(T - 300)) \quad (2)$$

where $V_{\text{glass}}(300 \text{ K})$ is the volume at 300 K, and α_{glass} is the thermal expansion coefficient of the glass. The uncertainties on $V_{\text{glass}}(T)$ derived from equation (2) are given by:

$$\Delta V_{\text{glass}}(T) = V_{\text{glass}}(T) (\Delta V_{\text{glass}}(300 \text{ K})/V_{\text{glass}}(300 \text{ K}) + (T - 300) \Delta \alpha_{\text{glass}} + \alpha_{\text{glass}} \Delta T) \quad (3)$$

From equation (3) the uncertainty in $\Delta V_g(T)$ is highest around the glass transition temperature T_g . The contribution of $\alpha_g \times \Delta T$ on $\Delta V_g(T)$ is so small that it can be neglected. For anhydrous glasses, the errors at T_g represent about 0.15 % of the molar volumes. For the hydrous glasses, the error is slightly higher, $\sim 0.20 \text{ cm}^3 \text{ mol}^{-1}$, which represents $\sim 0.7\%$ of volume at the glass transition temperature.

Volume of dry and hydrous silicate liquids

All experimental volumes with their corresponding uncertainties for hydrous and anhydrous samples are reported in Table 6. For liquids, the volume is given by:

$$V_{\text{liquid}}(T) = V_{\text{glass}}(T_g) \exp(\alpha_{\text{liquid}}(T - T_g)) \quad (4)$$

where T_g is the glass transition temperature, $V_{\text{glass}}(T_g)$, the volume at T_g is equal to $V_{\text{liquid}}(T_g)$ and α_{liquid} is the thermal expansion coefficient of the silicate liquid.

The uncertainties on these values are given by:

$$\Delta V_{\text{liquid}}(T) = V_{\text{liquid}}(T) (\Delta V_{\text{glass}}(T_g)/V_g(T_g) + (T - T_g) \Delta \alpha_{\text{liquid}}) \quad (5)$$

In the investigated temperature ranges the uncertainties on the supercooled liquid volumes are less than $0.2 \text{ cm}^3 \text{ mol}^{-1}$ which corresponds to about 0.7%. In equation (5) we assume $\Delta\alpha_g = \Delta\alpha_l = 5\%$ and we again consider that the contribution of $\alpha_{\text{liquid}} \Delta T$ to the error is too small to be taken into account. The uncertainties become unacceptably large if the data are extrapolated too far beyond the range of the measurements because of the $(T - T_g)$ term. For all compositions studied, the volume increases markedly on heating above the glass transition, and this increase is the highest for the highest water contents (*cf.* Fig. 3 a-c).

Table 5 lists the linear fits made to our experimental data for glasses and supercooled liquids with the following equations:

For glasses:
$$V_{\text{glass}} (\text{cm}^3 \text{ mol}^{-1}) = a_{\text{glass}} + \left(\frac{dV}{dT}\right)_{\text{glass}} T (\text{K}) \quad (6)$$

and for liquids:
$$V_{\text{liquid}} (\text{cm}^3 \text{ mol}^{-1}) = a_{\text{liquid}} + \left(\frac{dV}{dT}\right)_{\text{liquid}} T (\text{K}) \quad (7)$$

Liquid volumes were calculated by using the viscosimetric or calorimetric glass transition temperature as the starting point and the experimentally determined expansivity over temperature intervals of 50 K.

4. Discussion

Following Bottinga and Weill (1970), one generally assumes that the 1-bar partial molar volumes of oxides in silicate liquids do not depend on composition over a range of 40-80 mol% SiO₂. Therefore, the density of a silicate liquid can be expressed by the following equation (8):

$$\rho_{liquid}(T) = \frac{\sum X_i \times M_i}{V_{liquid}(T)}$$

where X_i is the mole fraction of oxide i , M_i its gram formula weight, and $V_{liquid}(T)$ is the volume of the silicate liquid at temperature T . Likewise, the molar volume of a melt is

$$V_{liquid}(T) = \sum X_i \times \left[\bar{V}_i(T_{ref}) + \frac{d\bar{V}_i}{dT} \times (T - T_{ref}) \right] \quad (9)$$

where $\bar{V}_i(T_{ref})$ is the partial molar volume of oxide i at reference temperature T_{ref} , and $\frac{d\bar{V}_i}{dT}$ is the partial molar thermal expansivity of oxide i .

At high pressure, an additional term needs to be included to deal with the compressibility of silicate liquid components (*e.g.* Lange 1994) so that equation (7) becomes:

$$V_{liquid}(T) = \sum X_i \times \left[\bar{V}_i(T_{ref}) + \frac{d\bar{V}_i}{dT} \times (T - T_{ref}) + \frac{d\bar{V}_i}{dP} \times (P - P_{ref}) \right] \quad (10)$$

where $\frac{d\bar{V}_i}{dP}$ is the partial molar compression of oxide i , P is the pressure and P_{ref} is the reference pressure (usually 1 bar). However, equation (10) cannot be extrapolated to GPa pressures because it does not account for the marked decrease of the compressibility with increasing pressures (Lange, 1994; Jing and Karato, 2009). Third-order Birch-Murnaghan equations of state have thus been used instead to describe the compression of volatile-bearing silicate melts (*e.g.* Jing and Karato, 2009; Malfait et al., 2014a,b).

The most widely used density/volume calculation model for hydrous silicate melts is the one proposed by Ochs and Lange (1999), which is an extension to hydrous liquids of

the model derived by Lange (1997) for anhydrous silicate melts from the glass transition to super-liquidus temperatures. Below, the experimentally determined volumes are compared with the predictions of the models of Lange (1997) and Ochs and Lange (1999) for anhydrous and hydrous supercooled melts, respectively.

Anhydrous supercooled silicate melts

As reported in Table 7, the model of Lange (1997) (with the partial molar volume for TiO_2 taken from Lange and Carmichael, 1987) reproduces the present volume data for most of the anhydrous melts to better than 1%, and trachyte volumes to about 1.3%. Hence these deviations are consistent with the stated uncertainties of the experimental data and of the model values.

The exception is the experimental dataset for the anhydrous foidite composition which is the least silicic and most calcic composition, containing about 43 mol% SiO_2 and 27.6 mol% CaO (Table 7). Equation (9), which is widely used to predict the volume of silicate melts at 1 bar, carries the assumption that molar volume follows a linear variation with composition. To explain the foidite anomaly, we first note that the volume data reported by Tomlinson et al. (1958) show a non-ideal mixing between CaO and SiO_2 in the binary system CaO-SiO_2 . Lange and Carmichael (1987) suggested an excess volume term between CaO and SiO_2 for silicate melts in the $\text{CaO-MgO-Al}_2\text{O}_3\text{-SiO}_2$ system having a molar fraction of $\text{CaO} > 0.5$. Courtial and Dingwell (1995) found a non-linear composition dependence of molar volume in the system $\text{CaO-Al}_2\text{O}_3\text{-SiO}_2$. Combining the model of Courtial and Dingwell (1999) valid for compositions in the system $\text{CaO-MgO-Al}_2\text{O}_3\text{-SiO}_2$, which includes an excess volume term between CaO and Al_2O_3 , with the partial molar volumes for TiO_2 , Na_2O and K_2O given by Lange (1997), reproduces the molar volume of

foidite composition within experimental uncertainties. The partial molar volumes for oxides used in all the calculations are given in Table 7.

Hydrous supercooled silicate melts

For hydrous silicate melts, the model of Ochs and Lange (1999) reproduces the present hydrous supercooled liquid volumes to within 1.15%. This agreement confirms that the partial molar of water ($\bar{V}_{\text{H}_2\text{O}}$) cannot depend strongly on the chemical composition of the silicate end-member. However, the agreement between our experimental data and the model of Ochs and Lange (1999) deteriorates with increasing water content (Table 7). To improve the prediction for our own experiments we derived new values for $\bar{V}_{\text{H}_2\text{O}}$ and $\frac{d\bar{V}_{\text{H}_2\text{O}}}{dT}$.

The starting point of this determination is the observation that, for all series of hydrous glasses, the trends in $\left(\frac{\partial V}{\partial T}\right)$ as a function of water content vary somewhat systematically with the NBO/T of the anhydrous end-member (Fig. 4a). The highly polymerized albite has a lower value of $0.70 \times 10^{-3} \text{ cm}^3 \text{ mol}^{-1} \text{ K}^{-1}$ compared to foidite, the most depolymerized composition, with a value of $1.51 \times 10^{-3} \text{ cm}^3 \text{ mol}^{-1} \text{ K}^{-1}$.

Considering all data, we observe that $\left(\frac{\partial V}{\partial T}\right)$ increases linearly with increasing water content, with partial molar values of $\frac{d\bar{V}_{\text{H}_2\text{O}}}{dT}$ between 14.3×10^{-3} and $17.5 \times 10^{-3} \text{ cm}^3 \text{ mol}^{-1} \text{ K}^{-1}$ for our set of compositions. As an approximation, a constant $\frac{d\bar{V}_{\text{H}_2\text{O}}}{dT}$ of $(15.9 \pm 1.6) \times 10^{-3} \text{ cm}^3 \text{ mol}^{-1} \text{ K}^{-1}$ could thus be assumed, a value 40% higher than the $(9.5 \pm 0.8) \times 10^{-3} \text{ cm}^3 \text{ mol}^{-1} \text{ K}^{-1}$ derived by Ochs and Lange (1999), as shown in Fig. 4b. We then used this new value for $\frac{d\bar{V}_{\text{H}_2\text{O}}}{dT}$ to determine a partial molar volume of $23.8 \pm 0.5 \text{ cm}^3 \text{ mol}^{-1}$ for water dissolved in silicate melt at a reference temperature of 1273 K.

This volume at 1273 K is 4% higher than that derived by Ochs and Lange (1999), and combined with our higher $\frac{d\bar{V}_{H_2O}}{dT}$, suggests that at 1473K the hydrous component in melts has a volume of 27.0 cm³ mol⁻¹ rather than 24.8 cm³ mol⁻¹. In arc basalts, which commonly contain ≥ 3 wt.% H₂O (~10 mol%), this difference between the two values translates to a difference of ~20-25 kg m⁻³ in the density of the liquid. Although a relatively small uncertainty in the overall magma density, of the order of 1%, this difference is equivalent to a pressure uncertainty of 1-2 kbars. Tholeiitic basalts are typically much drier, so the difference is smaller, of the order of 10 kg m⁻³ for 1 wt.% H₂O. However, even this small difference can be critical when calculating whether plagioclase crystals should be positively or negatively buoyant, as discussed by Ochs and Lange (1999).

Along with the partial molar volume and expansivity of other oxides reported by Lange (1997), the new values for water described above allow our data to be reproduced with a smaller error (see Table 7 for a comparison between both models). The present calibration covers water contents from 0 to about 3 wt% H₂O, and care should be exercised in extrapolating beyond this range. However it is notable that no previous study has detected any dependence of the partial molar volume properties of water (including compressibility and expansivity) on water content.

Effect of water on α_{glass} and α_{liquid}

The present thermal expansion coefficients of the silicate glasses and liquids are plotted against water content in Fig. 5a-b. Within its 5% estimated uncertainty α varies linearly with water content up to about 11 mol% H₂O for both kinds of phases. Note that from the definition of α as $\frac{1}{V} \frac{dV}{dT}$, it is impossible for α to be a linear function of water content if partial molar volumes and thermal expansivities are also additive, as assumed in equation 10 and supported by the available data. Over the measured range of three or four

water contents per base composition, the variations in α are most reasonably described as linear (Fig. 5). For hydrous glasses, all data show an expansivity increase as a function of water content, except for the trachyte series where an apparently slightly negative slope is found ($10^5 \alpha = 2.4738 - 0.01790 x_{\text{H}_2\text{O}}$). For the trachyte series, a linear extrapolation of the best fit of the data yields a value of $0.7 \times 10^{-5} \text{ K}^{-1}$ for the partial molar thermal expansion coefficient of water in glass. For the other compositions, the partial molar thermal expansion coefficient of H_2O in glass varies between $4.8 \times 10^{-5} \text{ K}^{-1}$ to $9.4 \times 10^{-5} \text{ K}^{-1}$. The results also point to a small pressure dependence of the expansivity as determined from the differences between the data for compacted and relaxed glasses, where compacted glasses show a higher expansivity (Table 5).

In summary, the average of the partial molar thermal expansion coefficient of water in silicate glasses is about $(6.2 \pm 3.5) \times 10^{-5} \text{ K}^{-1}$. This is consistent with several previous studies. Shelby and McVay (1976), Jewell et al. (1990) and Jewell and Shelby (1992) demonstrated the slight influence of water on thermal expansion for a variety of glasses containing 600 or 1850 ppm H_2O . The observations of Tomozawa et al. (1983) for hydrated $\text{Na}_2\text{Si}_3\text{O}_7$ glasses indicate that α_g is twice as great for a sample with 22 mol% H_2O than for the water-free glass, which corresponds to a mean coefficient of about $4 \times 10^{-5} \text{ K}^{-1}$ for the water component. This value is very similar to the figure of $6 \times 10^{-5} \text{ K}^{-1}$ derived from the data of Ochs and Lange (1997) for hydrous albite glasses. Although there is some scatter in the extrapolated values, there is no obvious systematic trend as a function of silicate composition.

For the liquids, all compositions show an increase of the thermal expansion coefficient as a function of water content. The derived partial molar thermal expansion coefficient of water for silicate melts range from 11×10^{-5} to $36 \times 10^{-5} \text{ K}^{-1}$, and the average of $\bar{\alpha}_{\text{H}_2\text{O}}^{\text{liq}}$ for the hydrous melts studied is about $(24.5 \pm 10) \times 10^{-5} \text{ K}^{-1}$. No systematic variation

of $\bar{\alpha}_{H_2O}^{liq}$ is observed with the NBO/T of the anhydrous end-members or any other characteristic of the silicate melt composition.

Configurational thermal expansion

The differences observed between the expansion of hydrated glasses and liquids reflect the existence of configurational contributions to the expansivities of the liquids, which are nonexistent in the glasses. Linear fits of molar volume ($\text{cm}^3 \text{mol}^{-1}$) and thermal expansivity of glasses and supercooled liquids in the albite, tephrite, trachyte and foidite hydrous compositions are reported in Table 8. Because no compositional effects were observed for thermal expansion of glasses, as discussed above, the complexities affecting melts must find their roots in the structural changes that begin to take place at the glass transition. As discussed for the heat capacity or viscosity (*e.g.* Bouhifd et al., 1998; Richet, 1984; and references therein), the thermal expansivity of silicate liquids is made up of vibrational and configurational parts. Hence one can write that:

$$\frac{dV_i}{dT} = \frac{dV_i^{vib}}{dT} + \frac{dV_i^{conf}}{dT} \quad (11)$$

where $\frac{dV_i^{vib}}{dT}$ and $\frac{dV_i^{conf}}{dT}$ are the vibrational and configurational contributions, respectively, to $\frac{dV_i}{dT}$. The abrupt jump in thermal expansivity at the glass transition reflects the contribution of $\frac{dV_i^{conf}}{dT}$.

Combining the results for the present glass compositions except the hydrous trachyte series we find that $\frac{dV_i^{vib}}{dT}$ is $(1.5 \pm 0.5) \times 10^{-3} \text{ cm}^3 \text{mol}^{-1} \text{K}^{-1}$ for the water component. With respect to this vibrational contribution to expansivity, water behaves similarly to alkali oxides, with a partial molar value between that of Li_2O and Na_2O (Shelby and McVay, 1976; Richet et al., 2000).

For the configurational contribution to expansivity, we find two distinct trends versus the water contents of the liquids: one for polymerized and the other for depolymerized compositions (Fig. 6). For instance, for the three compositions with $\text{NBO}/\text{T} \leq 0.21$, a positive slope of $\frac{dV_i^{\text{conf}}}{dT}$ versus water content is observed. In contrast, a negative slope is observed for the most depolymerized compositions with NBO/T of 0.86 and 1.51 (for the anhydrous end-member). This contrast is consistent with other effects of dissolved water that behave differently depending for polymerized or depolymerized compositions, at least at atmospheric pressure. For instance, the partial molar heat capacity of OH^- for depolymerized melts is close to double the value for polymerized melts (Bouhifd et al., 2013). Likewise the addition of water increases the Poisson's ratio for polymerized melts, but decreases it for depolymerized melts (Malfait and Sanchez-Valle, 2013). All these features thus support the idea that the solubility mechanisms of water strongly depend on silicate composition and polymerization (*e.g.* Kohn, 2000; Mysen and Richet, 2005; Xue and Kanzaki, 2006; Malfait and Sanchez-Valle, 2013; Robert et al., 2014; and references therein). The fascinating enigma remains that despite this conclusion, the partial molar properties of the dissolved hydrous component clearly do not depend on water speciation.

5. Conclusion

The $\bar{V}_{\text{H}_2\text{O}}$ at atmospheric pressure can be considered as independent of silicate composition in glasses, and in supercooled liquids near the glass transition temperature, as reported previously by Richet et al. (2000), and Ochs and Lange (1999) and Bouhifd et al. (2001), respectively. This behaviour seems to be valid too at high pressure (up to about 20 GPa) (*e.g.* Malfait et al., 2014b; and references therein). This uniform volume of dissolved water in silicate melts will simplify the construction of general density model for H_2O bearing magmas at high pressure and high temperature. However, contrasting trends are

observed in this study for the configurational contributions to the expansivity with a positive slope of $\frac{dV_i^{conf}}{dT}$ versus water for the most polymerized compositions and a negative slope for the two most depolymerized compositions. Measurements at high water contents and high temperatures are needed to explore these effects further, and to determine their importance for magmas inside the Earth.

Acknowledgments. This work has been partly supported by the EU TMR network ERBFMRX 960063 “In situ hydrous melts.” M.A. Bouhifd acknowledges the support of “ClerVolc program” (the French Government Laboratory of Excellence initiative n°ANR-10-LABX-0006, the Région Auvergne and the European Regional Development Fund. This is Laboratory of Excellence ClerVolc contribution number 133). This research was also supported by the National Science Foundation through award EAR-0748411 to A.G. Whittington. We thank Carmen Sanchez-Valle and Rebecca Lange and two anonymous reviewers for constructive and helpful criticisms.

410 **References**

- 411 Agee, C. B., 2008. Compressibility of water in magma and the prediction of density
 412 crossovers in mantle differentiation. *Philosophical Transactions of the Royal Society, A*,
 413 366, 4239-4252.
- 414
- 415 Behrens, H., Romano, C., Nowak, M., Holtz, F., Dingwell, D.B., 1996. Near-infrared
 416 spectroscopic determination of water species in glasses of the system MAlSi_3O_8 (M = Li,
 417 Na, K): an interlaboratory study. *Chemical Geology* 128, 41-63.
- 418
- 419 Bottinga, Y., Weill, D.F., 1970. Densities of liquid silicate systems calculated from partial
 420 molar volumes of oxide components. *American Journal of Science* 269, 169-182.
- 421
- 422 Bottinga, Y., Weill, D.F., Richet, P., 1982. Density calculations for silicate liquids. I. Revised
 423 method for aluminosilicate compositions. *Geochimica et Cosmochimica Acta* 46, 909-919.
- 424
- 425 Bouhifd, M.A., Courtial, P., Richet, P., 1998. Configurational heat capacities: alkali vs.
 426 alkaline-earth aluminosilicate liquids. *Journal of Non-Crystalline Solids* 231, 169-177.
- 427
- 428 Bouhifd, M.A., Whittington, A., Richet, P., 2001. Partial molar volume of water in phonolitic
 429 glasses and liquids. *Contributions to Mineralogy and Petrology* 142, 235-243.
- 430
- 431 Bouhifd, M.A., Whittington, A., Roux, J., Richet, P., 2006. Effect of water on the heat
 432 capacity of polymerized aluminosilicate melts. *Geochimica et Cosmochimica Acta* 70,
 433 711-722.
- 434
- 435 Bouhifd, M.A., Whittington, A.G., Withers, A.C., Richet, P., 2013. Heat capacities of hydrous
 436 silicate glasses and liquids. *Chemical Geology* 346, 125-134.
- 437
- 438 Burnham, C.W., Davis, N.F., 1971. The role of H_2O in silicate melts: I. P-V-T relations in the
 439 system $\text{NaAlSi}_3\text{O}_8$ - H_2O to 10 kilobars and 1000 °C. *American Journal of Science* 270, 54-
 440 79.
- 441
- 442 Courtial, P., Dingwell, D.B., 1995. Non-linear composition dependence of molar volume of
 443 melts in the $\text{CaO-Al}_2\text{O}_3\text{-SiO}_2$ system. *Geochimica et Cosmochimica Acta* 59, 3685-3695.
- 444
- 445 Courtial, P., Dingwell, D.B., 1999. Densities of melts in the $\text{CaO-MgO-Al}_2\text{O}_3\text{-SiO}_2$ system.
 446 *American Mineralogist* 84, 465-476.
- 447
- 448 Haggerty, J.S., Cooper, A.R., Heasley, J.H., 1968. Heat capacity of three inorganic glasses
 449 and liquids and supercooled liquids. *Physics and Chemistry of Glasses* 9, 47-51.
- 450
- 451 Jing, Z., Karato, S., 2009. The density of volatile bearing melts in the earth's deep mantle:
 452 The role of chemical composition. *Chemical Geology* 262, 100-107.
- 453
- 454 Jewell, J.M., Shelby, J.E., 1992. Effects of water on the properties of sodium aluminosilicate
 455 glasses. *Journal of American Ceramic Society* 75, 878-883.
- 456
- 457 Jewell, J.M., Spess, M.S., Shelby, J.E., 1990. Effects of water concentration on the properties
 458 of commercial soda-lime-silica glasses. *Journal of American Ceramic Society* 73, 132-135.

- Knoche, R., Dingwell, D.B., Webb, S.L., 1995. Leucogranitic and pegmatitic melt densities: partial molar volumes for SiO_2 , Al_2O_3 , Na_2O , K_2O , Rb_2O , Cs_2O , Li_2O , BaO , SrO , CaO , MgO , TiO_2 , B_2O_3 , P_2O_5 , F_2O_{-1} , Ta_2O_5 , Nb_2O_5 , and WO_3 . *Geochimica et Cosmochimica Acta* 59, 4645-4652.
- Kohn, S.C., 2000. The dissolution mechanisms of water in silicate melts: a synthesis of recent data. *Mineralogical Magazine* 64, 389-408.
- Lange, R.A., 1994. The effects of H_2O , CO_2 and F on the density and viscosity of silicate melts. *Reviews in Mineralogy* 30, 331-369.
- Lange, R.A., 1997. A revised model for the density and thermal expansivity of K_2O - Na_2O - CaO - MgO - Al_2O_3 - SiO_2 liquids from 700 to 1900 K: extension to crustal magmatic temperatures. *Contributions to Mineralogy and Petrology* 130, 1-11.
- Lange, R.A., Carmichael, I.S.E., 1987. Densities of Na_2O - K_2O - CaO - MgO - FeO - Fe_2O_3 - Al_2O_3 - TiO_2 - SiO_2 liquids: New measurements and derived partial molar properties. *Geochimica et Cosmochimica Acta* 51, 2931-2946.
- Liu, Y., Nekvasil, H., Long, H., 2002. Water dissolution in albite melts: constraints from *ab initio* NMR calculations. *Geochimica et Cosmochimica Acta* 66, 4149-4163.
- Malfait, W.M., Sanchez-Valle, C., 2013. Effect of water and network connectivity on glass elasticity and melt fragility. *Chemical Geology* 346, 72-80.
- Malfait, W.M., Sanchez-Valle, C., Ardia, P., Médard, E., Lerch, P., 2011. Compositional dependent compressibility of dissolved water in silicate glasses. *American Mineralogist* 96, 1402-1409.
- Malfait, W.M., Seifert, R., Petitgirard, S., Perrillat, J-P., Mezouar, M., Ota, T., Nakamura, E., Lerch, P., Sanchez-Valle, C., 2014a. Supervolcano eruptions driven by melt buoyancy in large silicic magma chambers. *Nature Geoscience* 7, 122-125.
- Malfait, W.M., Seifert, R., Petitgirard, S., Mezouar, M., Ota, T., Sanchez-Valle, C., 2014b. The density of andesitic melts and the compressibility of dissolved water in silicate melts at crustal and upper mantle conditions. *Earth and Planetary Science Letters* 393, 31-38.
- Mysen, B.O., Acton, M., 1999. Water in H_2O -saturated magma-fluid systems: Solubility behavior in K_2O - Al_2O_3 - SiO_2 - H_2O to 2.0 GPa and 1300 °C. *Geochimica et Cosmochimica Acta* 63, 3799-3815.
- Mysen, B.O., Richet, P., 2005. *Silicate Glasses and Melts: Properties and Structure*. Elsevier, Amsterdam.
- Mysen, B.O., Wheeler, K., 2000. Solubility behavior of water in haploandesitic melts at high pressure and high temperature. *American Mineralogist* 85, 1128-1142.

- Nowak, M., Behrens, H., 1995. The speciation of water in haplogranitic glasses and melts determined by *in situ* near-infrared spectroscopy. *Geochimica et Cosmochimica Acta* 59, 3445-3450.
- Ochs, F.A., Lange, R.A., 1997. The partial molar volume, thermal expansivity, and compressibility of H₂O in NaAlSi₃O₈ liquid: new measurements and an internally consistent model. *Contributions to Mineralogy and Petrology* 129, 155-165.
- Ochs, F.A., Lange, R.A., 1999. The density of hydrous magmatic liquids. *Science* 283, 1314-1317.
- Richet, P., 1984. Viscosity and configurational entropy of silicate melts. *Geochimica et Cosmochimica Acta* 48, 471-483.
- Richet, P., Lejeune, A.M., Holtz, F., Roux, J., 1996. Water and the viscosity of andesite melts. *Chemical Geology* 128, 185-197.
- Richet, P., Polian, A., 1998. Water as a dense icelike component in silicate glasses. *Science* 281, 396-398.
- Richet, P., Whittington, A., Holtz, F., Behrens, H., Ohlhorst, S., Wilke, M., 2000. Water and the density of silicate glasses. *Contributions to Mineralogy and Petrology* 138, 337-347.
- Robert, E., Whittington, A., Fayon, F., Pichavant, M., Massiot, D., 2001. Structural characterization of water-bearing silicate and alumino-silicate glasses by high resolution solid state NMR. *Chemical Geology* 174, 291-305.
- Robert, G., Whittington, A., Stechern, A., Behrens, H., 2014. Heat capacity of hydrous basaltic glasses and liquids. *Journal of Non-Crystalline Solids* 390, 19-30.
- Schmidt, B.C., Riemer, T., Kohn, S.C., Holtz, F., Dupree, R., 2001. Structural implications of water dissolution in haplogranitic glasses from NMR spectroscopy: influence of total water content and mixed alkali effect. *Geochimica et Cosmochimica Acta* 65, 2949-2964.
- Shelby, J.E., McVay, G.L., 1976. Influence of water on the viscosity and thermal expansion of sodium trisilicate glasses. *Journal of Non-Crystalline Solids* 20, 439-449.
- Shen, A., Keppler, H., 1995. Infrared spectroscopy of hydrous silicate melts to 1000 °C and 10 kbar - direct observation of H₂O speciation in a diamond-anvil cell. *American Mineralogist* 80, 1335-1338.
- Silver, L.A., Ihinger, P.D., Stolper, E., 1990. The influence of bulk composition on the speciation of water in silicate glasses. *Contributions to Mineralogy and Petrology* 104, 142-162.
- Sipp, A., Richet, P., 2002. Kinetics of volume, enthalpy and viscosity relaxation in glass-forming liquids. *Journal of non-Crystalline Solids* 298, 202-212.

- Sowerby, J.R., Keppler, H., 1999. Water speciation in rhyolitic melt determined by *in-situ* infrared spectroscopy. *American Mineralogist* 84, 1843-1849.
- Stolper, E., 1982. Water in silicate glasses: an infrared spectroscopic study. *Contributions to Mineralogy and Petrology* 81, 1-17.
- Tomlison, J.W., Heynes, M.S.R., Bockris, J.O.M., 1958. The structure of liquid silicates: Part 2. Molar volumes and expansivities. *Transactions Faraday Society* 54, 1822-1833.
- Tomozawa, M., Takata, M., Acocella, J., Watson, E.B., Takamori, T., 1983. Thermal properties of $\text{Na}_2\text{O} \cdot 3\text{SiO}_2$ glasses with high water content. *Journal of Non-Crystalline Solids* 56, 343-348.
- Toplis, M.J., Richet, P. 2000. Equilibrium density and expansivity of silicate melts in the glass transition range. *Contributions to Mineralogy and Petrology* 139, 672-683.
- Whittington, A.G., Bouhifd, M.A., Richet, P., 2009. The viscosity of hydrous $\text{NaAlSi}_3\text{O}_8$ and granitic melts: Configurational entropy models. *American Mineralogist* 94, 1-16.
- Whittington, A., Richet, P., Behrens, H., Holtz, F., Scaillet, B., 2004. Experimental temperature- $\text{X}(\text{H}_2\text{O})$ -viscosity relationship for leucogranites and comparison with synthetic silicate liquids. *Transactions of the Royal Society of Edinburgh: Earth Sciences* 95, 59-71.
- Whittington, A., Richet, P., Polian, A., 2012. Water and the compressibility of silicate glasses: a Brillouin spectroscopic study. *American Mineralogist* 97, 455-467.
- Whittington, A., Richet, P., Holtz, F., 2000. Water and the viscosity of depolymerized aluminosilicate melts. *Geochimica et Cosmochimica Acta* 64: 3725-3736.
- Whittington, A., Richet, P., Linard, Y., Holtz, F., 2001. The viscosity of hydrous phonolites and trachytes. *Chemical Geology* 174, 209-223.
- Xue, X.Y., Kanzaki, M., 2004. Dissolution mechanisms of water in depolymerized silicate melts: Constraints from ^1H and ^{29}Si NMR spectroscopy and *ab initio* calculations. *Geochimica et Cosmochimica Acta* 68, 5027-5057.
- Xue, X.Y., Kanzaki, M., 2006. Depolymerization effect of water in aluminosilicate glasses: Direct evidence from ^1H - ^{27}Al heteronuclear correlation NMR. *American Mineralogist* 91, 1922-1926.

Figure Captions

Figure 1. Difference between the expansion of compacted and relaxed glasses at a heating rate of 2 K min⁻¹ for the sample “Trach 3.5” sample containing about 10 mol. % H₂O, which was synthesized at 3 kbar and 1300 °C. Note that a constant slope is observed up to T_{13} (temperature at which the viscosity is 10¹³ Pa.s) once a sample hydrated at a high pressure has relaxed to the 1-bar configuration.

Figure 2. Variations of sample lengths in natural logarithm with temperature for anhydrous and hydrated tephrite liquids. (a) Anhydrous tephrite liquid between 880 and 920 K; (b) Teph 0.3 liquid (1.74 mol% H₂O) between 820 and 860 K; (c) Teph 1.5 liquid (5.22 mol% H₂O) between 750 and 800 K; (d) Teph 3 liquid (8.31 mol% H₂O) between 670 and 740 K. Vertical scales change between panels because the thermal expansion of hydrous liquids increases at higher water contents.

Figure 3. Molar volumes in the glass transition range for hydrous trachyte glasses and supercooled liquids. (a) Anhydrous trachyte glass and liquid; (b) Trach 1.5 (5.42 mol% H₂O) glass and liquid; (c) Trach 3.5 (10.12 mol% H₂O) glass and liquid. The studied temperature ranges are lower for higher water contents since the glass transition temperature decreases with increasing water content.

Figure 4. Thermal expansivity of hydrous melts versus water content (mol%). (a) Experimental results up to about 11 mol%. (b) Extrapolation of the thermal expansivity to water end-member. These extrapolations lead to $\frac{d\bar{V}_{H_2O}}{dT} = 15.9 \pm 1.6 \text{ cm}^3 \text{ mol}^{-1} \text{ K}^{-1}$.

Figure 5. Coefficients of thermal expansion of hydrous (a) glasses; (b) liquids. All compositions (apart from the hydrous trachyte glasses) show an increase of the coefficient of thermal expansion with increasing water content.

Figure 6. Configurational contribution to expansivity for anhydrous and hydrous liquids studied in this work. The results for phonolite previously reported by Bouhifd et al. (2001) are also shown. Two different trends are observed: one for the polymerized hydrous melts (with NBO/T ≤ 0.21), and the second one for depolymerized melts (with an NBO/T ≥

629 0.86). For polymerized hydrous melts, an increase of $\frac{dV_i^{conf}}{dT}$ versus water content is
630 observed, whereas the opposite trend is observed for depolymerized melts.
631

Figure

Figure 1.

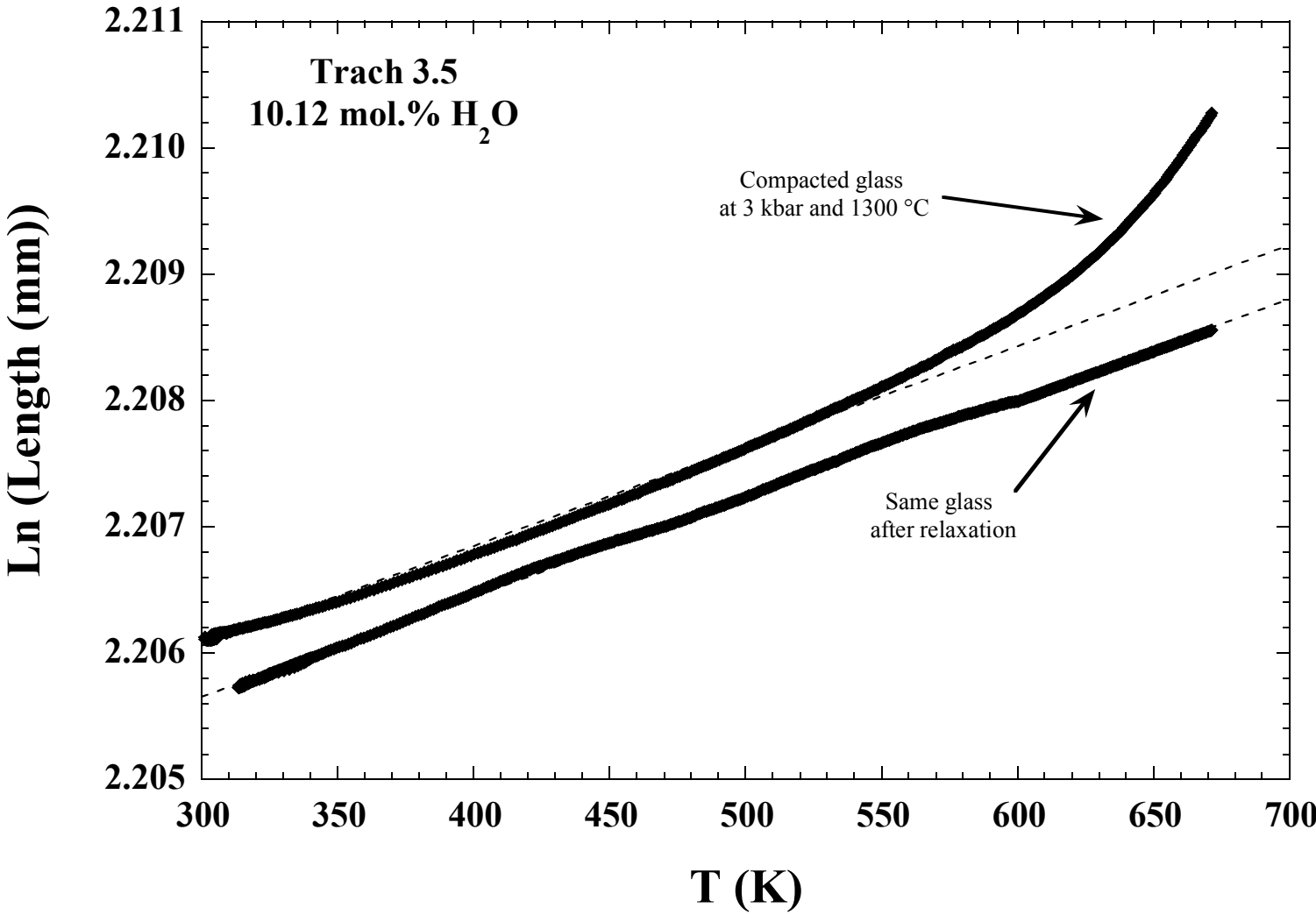


Figure 2.

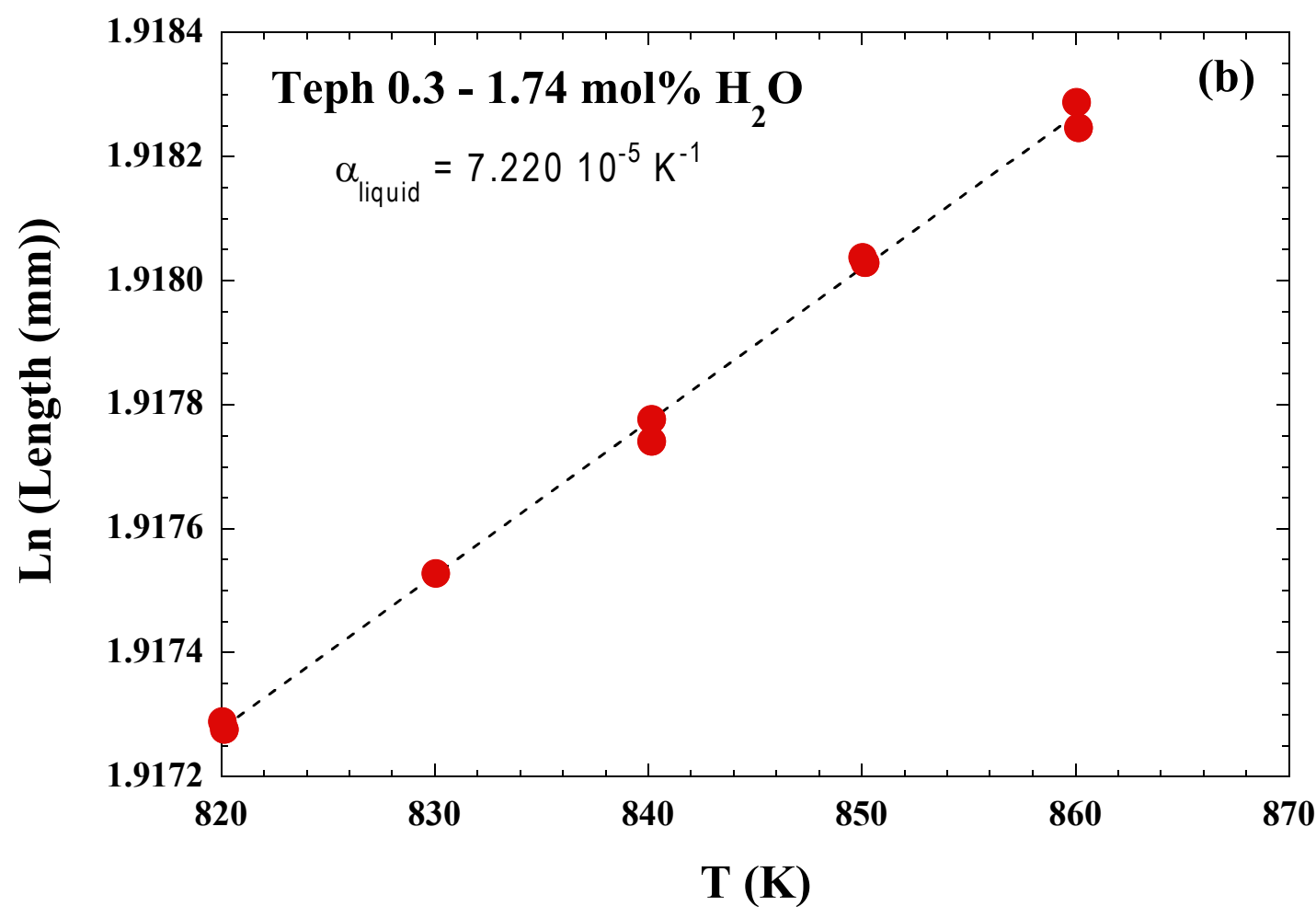
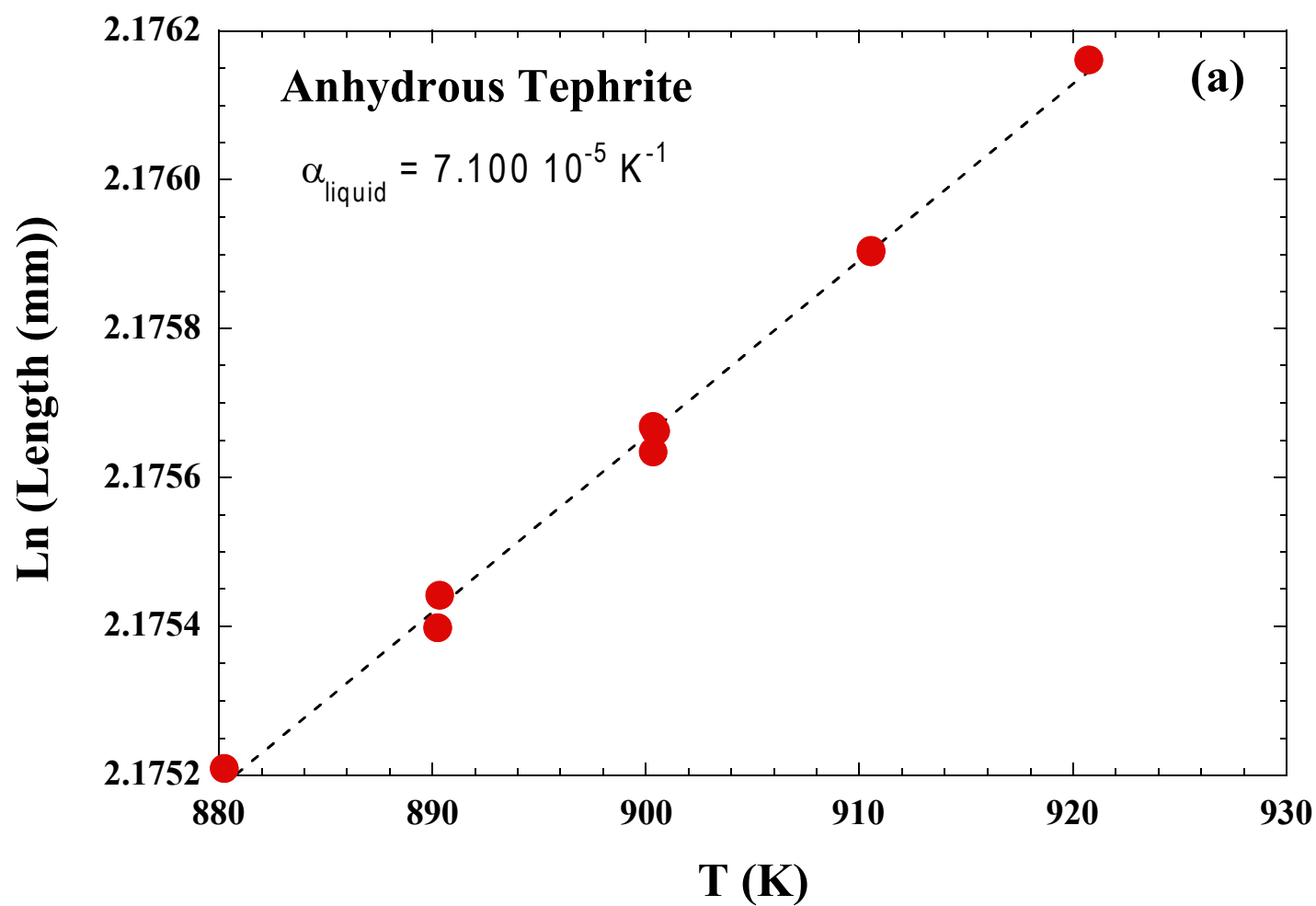


Figure 2.

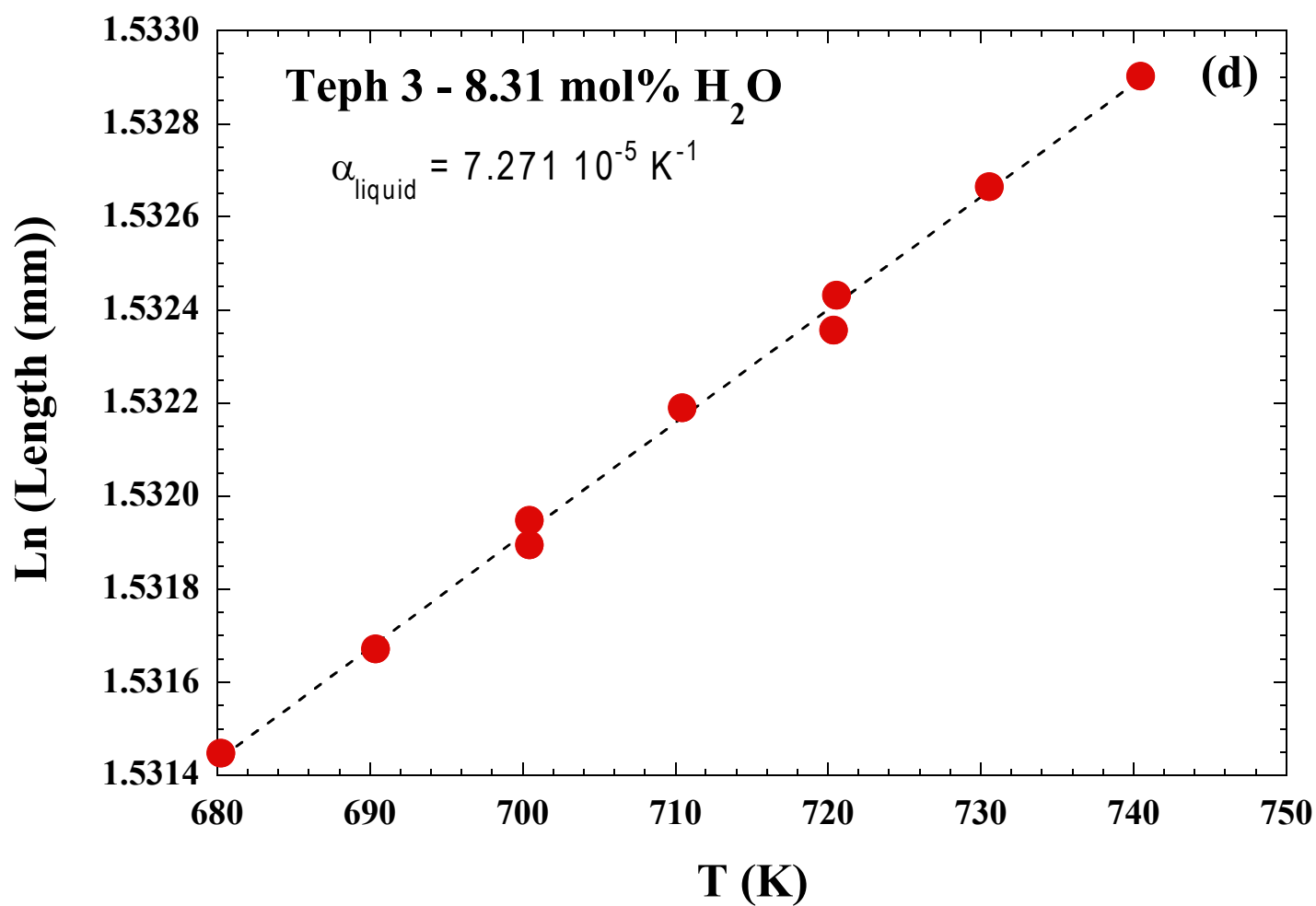
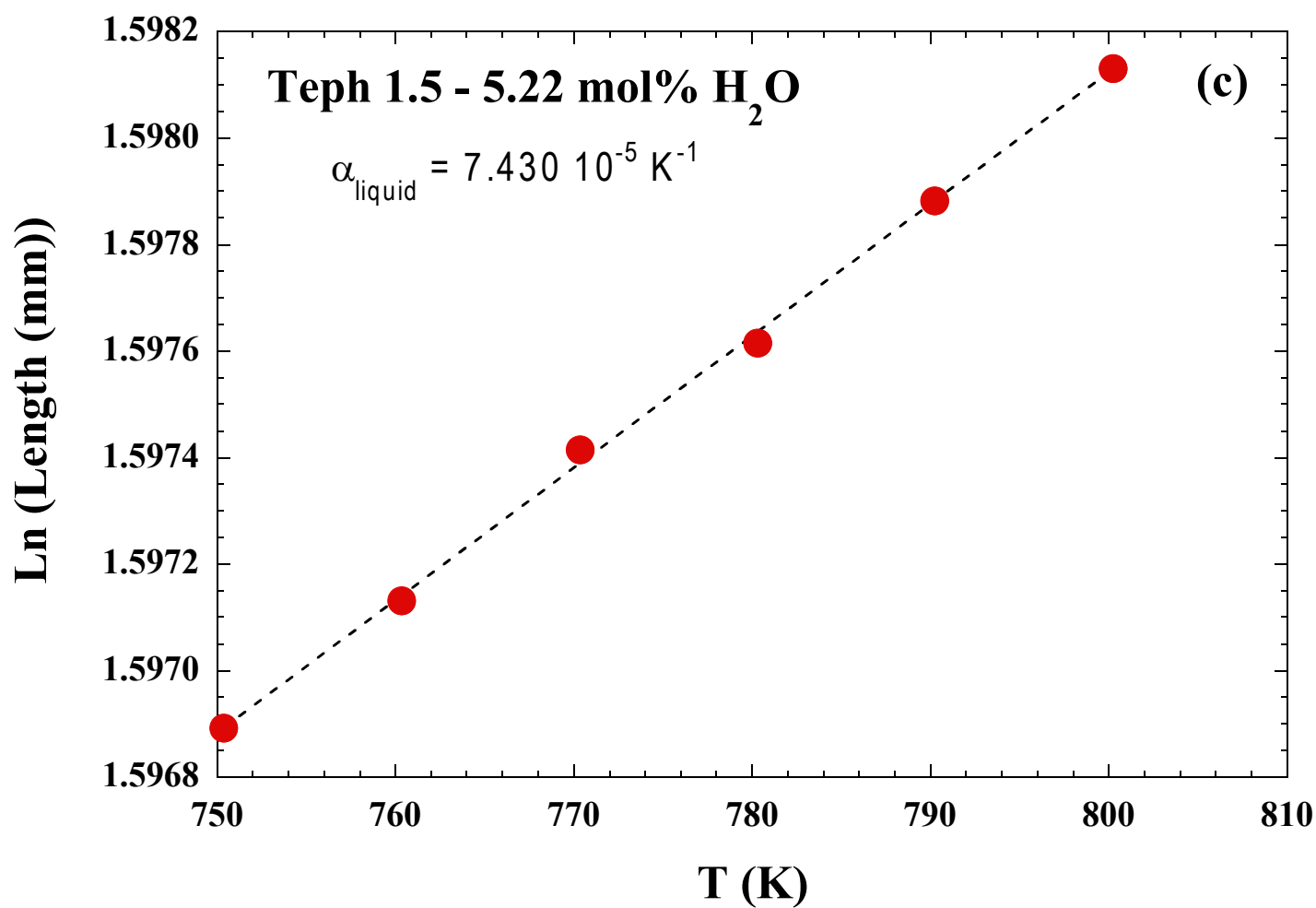


Figure 3.

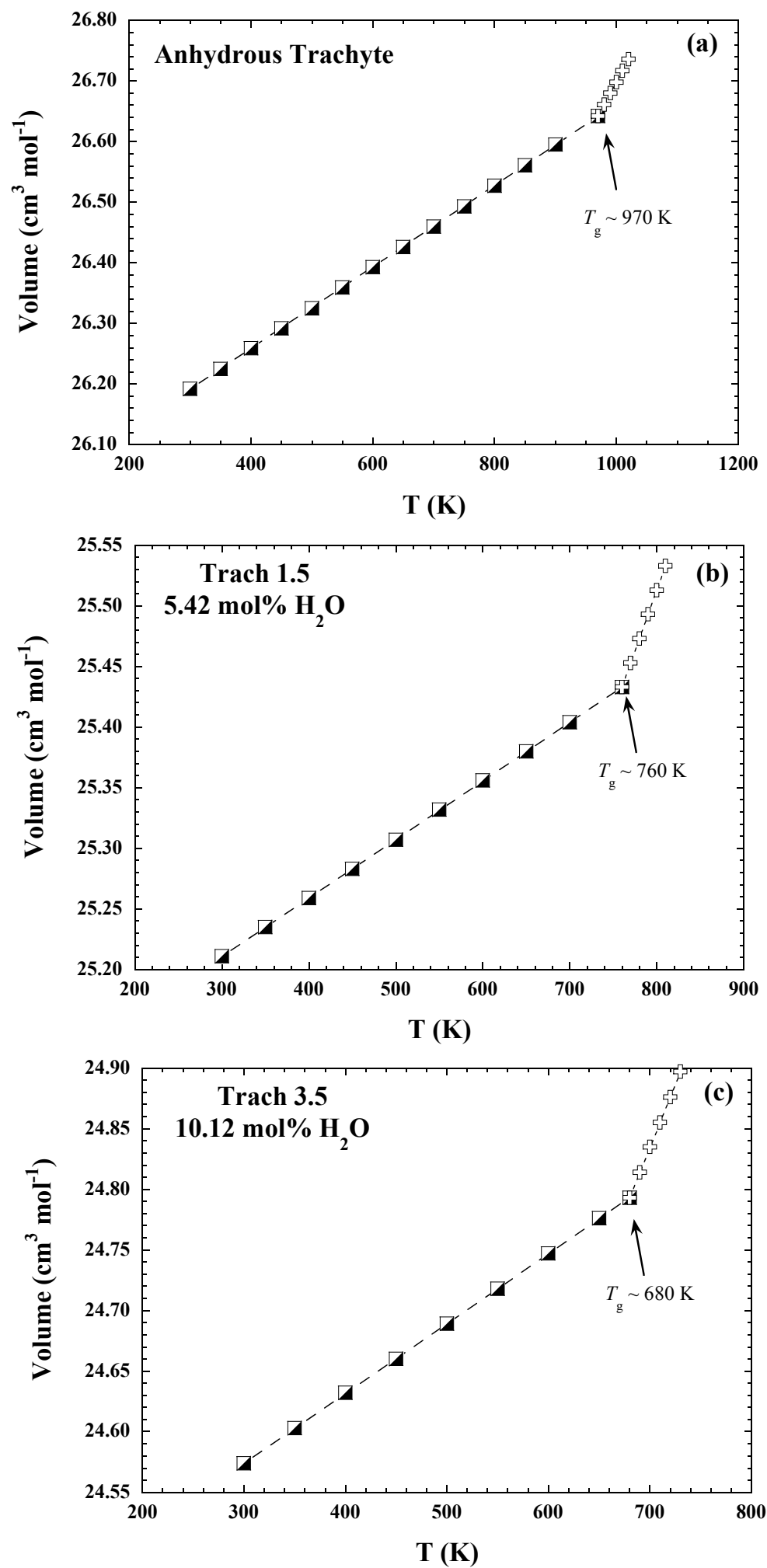


Figure 4.

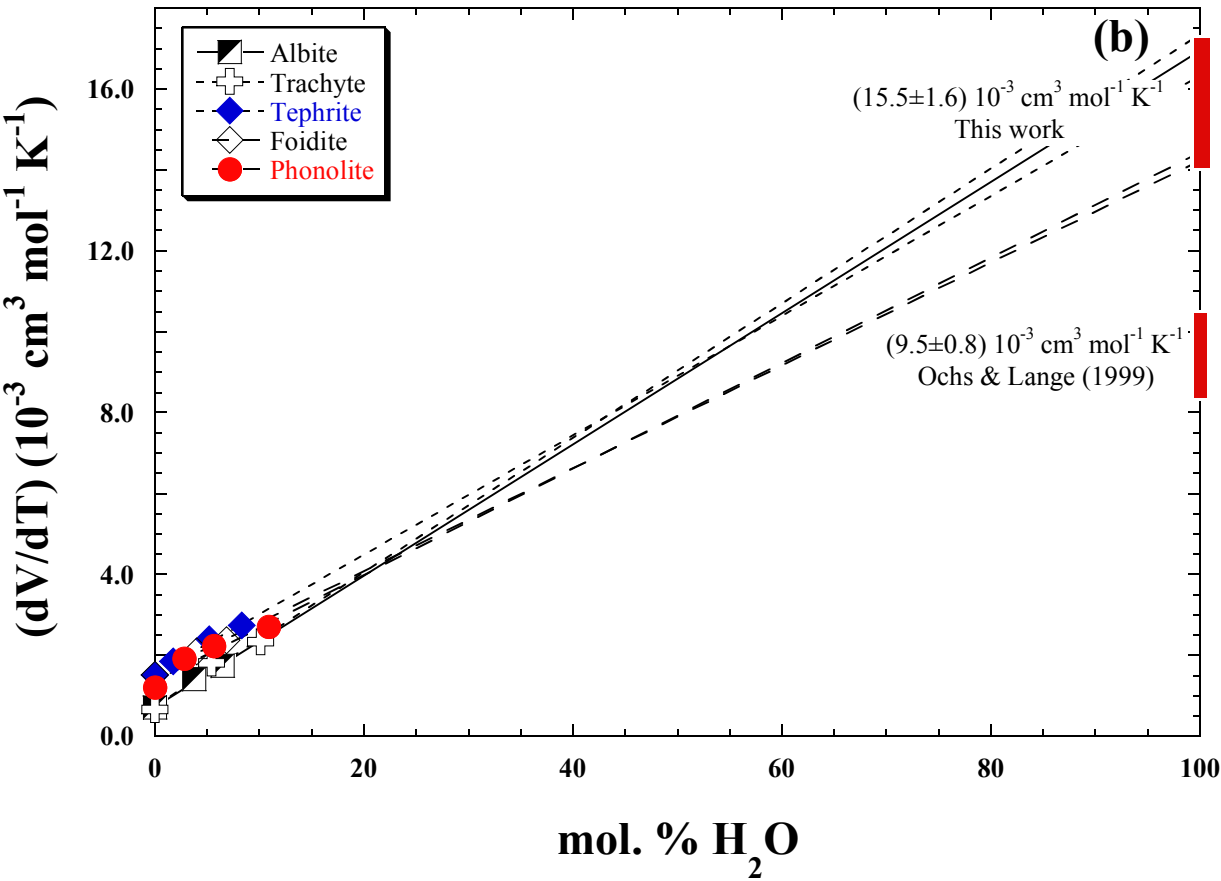
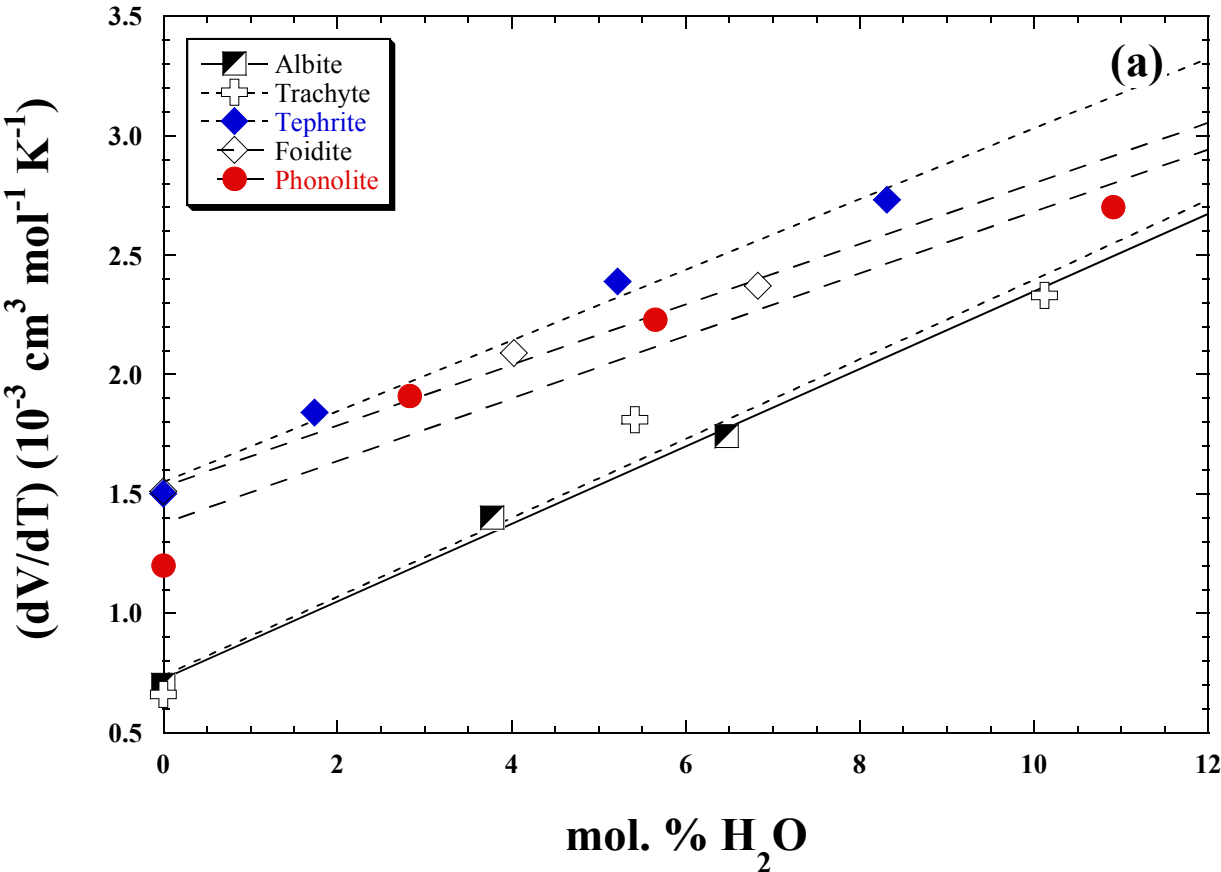


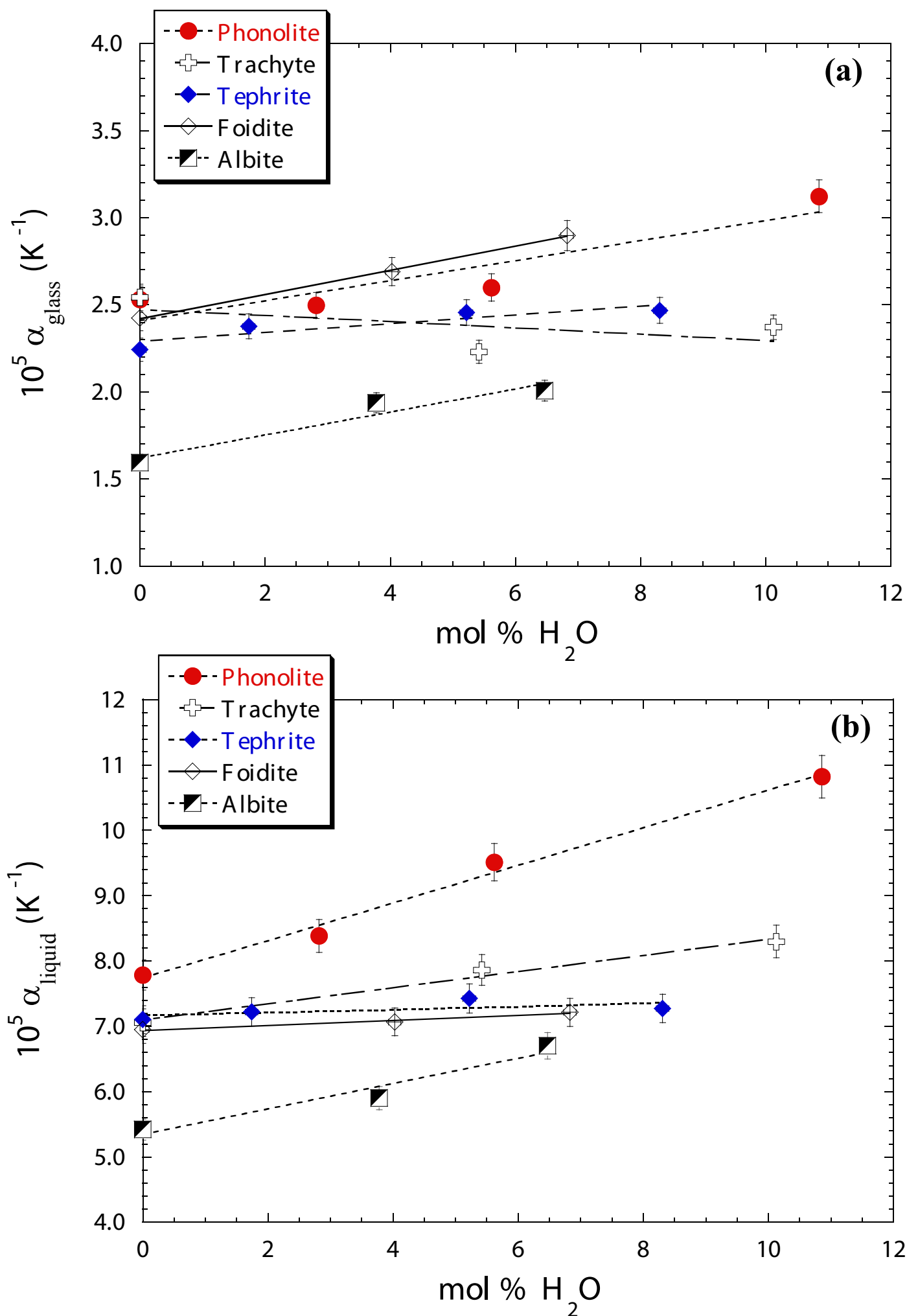
Figure 5.

Figure 6.

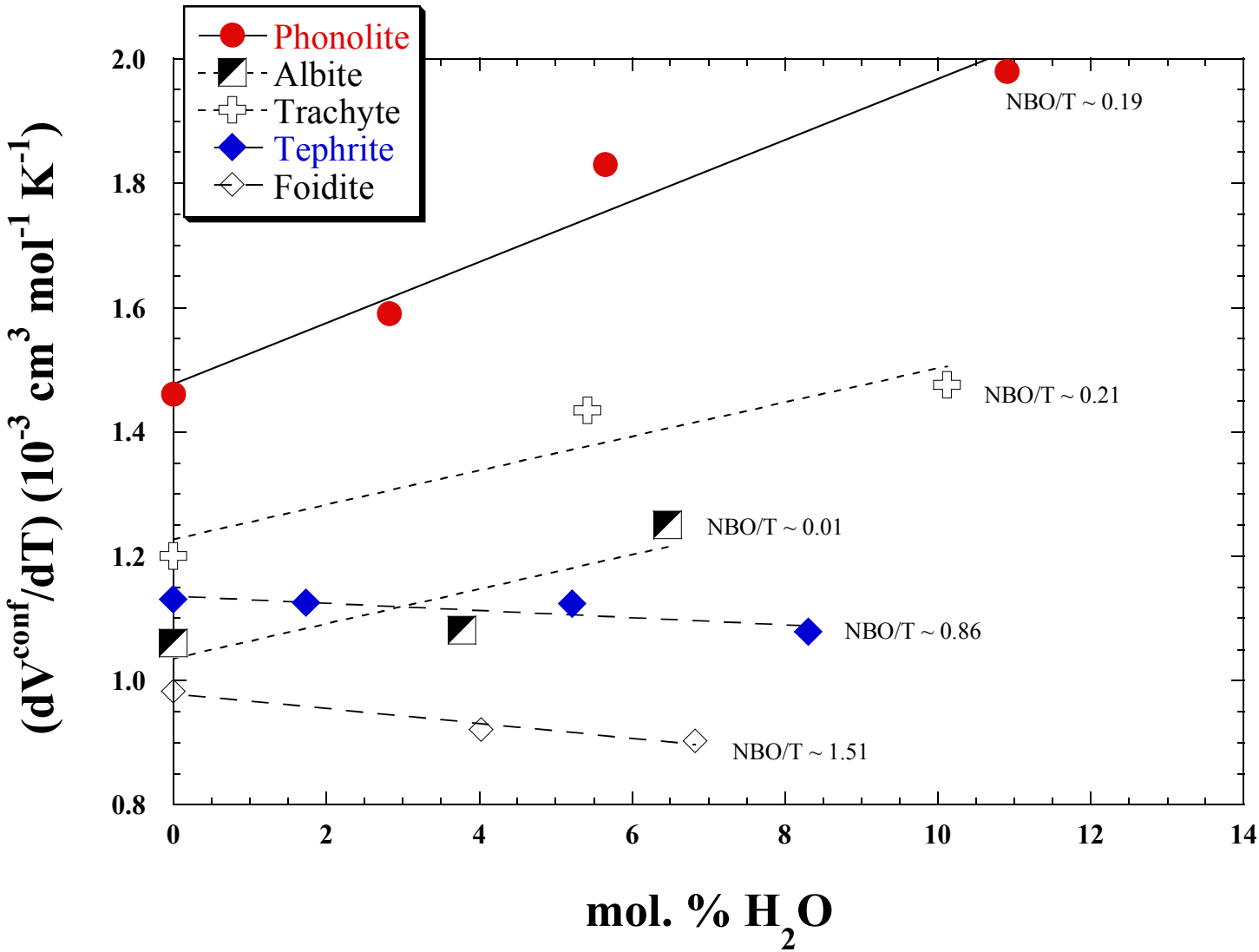


Table 1. Starting anhydrous compositions normalized to mole percent (mol%).

	Albite	Tephrite	Trachyte	Foidite	Phonolite ^a
SiO ₂	75.30	51.32	69.00	42.98	65.40
Al ₂ O ₃	12.07	8.39	10.54	5.92	12.72
Na ₂ O	12.62	6.93	6.95	7.26	10.03
K ₂ O	0.01	1.95	2.30	0.60	5.28
CaO		16.31	6.15	27.55	2.80
MgO		13.30	4.66	13.48	3.10
TiO ₂		1.79	0.40	2.20	0.66
gfw (g) ^b	65.381	61.468	64.324	59.573	66.810
N ^c	3.242	2.872	3.103	2.708	3.196
NBO/T ^d	0.01	0.86	0.21	1.51	0.19

^aThe experimental results for phonolite hydrous compositions are reported in Bouhifd et al. (2001).
^bGram formula weight on the basis of one mole of oxides.
^cN is the number of atoms per gfw.
^dNon-Bridging Oxygen per Tetrahedra cations ratio.

Table 2. Hydration conditions, water contents and densities of hydrated albite, tephrite, trachyte and foidite glasses.

Sample	H ₂ O ^a mol%	P (kbar)	T (°C)	t (h)
Albite				
Alb 0.				
Albite-1.3	3.78	2	1200	65
Albite-2.2	6.47	2	1200	65
Tephrite				
Teph 0.				
Teph 0.3	1.74	2	1300	18
Teph 1.5	5.22	3	1300	48
Teph 3	8.31	3	1300	45
Trachyte				
Trach 0.				
Trach 1.5	5.42	2	1300	18
Trach 3.5	10.12	3	1300	48
Foidite				
NIQ 0.				
NIQ 1.2	4.03	3	1300	18
NIQ 2.3	6.83	3	1300	18

^aWater content measured by Karl-Fischer titration (Whittington *et al.*, 2000).

Table 3. Water contents (mol%), gram formula weight on the basis of one mole of oxides, densities of compacted and relaxed glasses, and the corresponding 1 bar volumes.

Sample	H ₂ O mol%	gfw (g)	ρ_{comp} (g/cm ³)	V ₀ (comp) (cm ³ /mol)	ρ_{relax} (g/cm ³)	V ₀ (relax) (cm ³ /mol)	^a Diff%
Albite							
Alb 0.	0.0	65.385			2.371	27.577	
HAB0.6	2.39	64.249	2.387	26.916	2.376	27.041	0.46
Albite-1.3	3.78	63.596	2.384	26.676	2.373	26.800	0.46
Albite-2.2	6.47	62.322	2.375	26.241	2.366	26.341	0.38
HAB5.2	15.75	57.920	2.345	24.699	2.335	24.805	0.43
Tephrite							
Teph 0.	0.0	61.468			2.677	22.962	
Teph 0.3	1.74	60.712	2.686	22.603	2.677	22.679	0.34
Teph 0.8	2.92	60.200	2.682	22.446	2.671	22.538	0.41
Teph 1.8	4.46	59.530	2.674	22.263	2.661	22.371	0.49
Teph 1.5	5.22	59.201	2.677	22.115	2.664	22.223	0.49
Teph 2.2	7.29	58.301	2.661	21.909	2.644	22.050	0.64
Teph 3	8.31	57.855	2.656	21.783	2.644	21.882	0.45
Trachyte							
Trach 0.	0.0	64.328			2.456	26.192	
Trach 50	2.01	63.399	2.477	25.595	2.466	25.709	0.44
Trach 0.83	2.90	62.985	2.468	25.521	2.452	25.687	0.65
Trach 1.19	4.12	62.419	2.461	25.363	2.429	25.697	1.30
Trach 1.5	5.42	61.818	2.467	25.058	2.452	25.211	0.61
Trach 2.2	7.40	60.901	2.457	24.787	2.429	25.072	1.14
Trach 3.5	10.12	59.641	2.437	24.473	2.427	24.574	0.41
Trach 5	15.59	57.121	2.412	23.682	2.398	23.820	0.58
Foidite							
NIQ 0.	0.0	59.573			2.808	21.215	
NIQ 0.7	2.20	58.658	2.815	20.838	2.806	20.904	0.32
NIQ 1.	3.22	58.237	2.806	20.754	2.795	20.836	0.39
NIQ 1.2	4.03	57.899	2.801	20.671	2.790	20.752	0.39
NIQ 1.8	5.93	57.110	2.791	20.462	2.791	20.462	0.0
NIQ 2.3	6.83	56.736	2.789	20.343	2.766	20.512	0.83
Phonolite							
Phon 0.	0.0	66.810			2.457	27.192	
Phon 0.5B	0.78	65.428	2.472	24.468	2.464	26.554	0.32
Phon 1.6	5.65	64.052	2.460	26.037	2.458	26.059	0.08
Phon 2.2	7.53	63.135	2.458	25.686	2.450	25.769	0.33
Phon 3.2	10.91	61.486	2.438	25.220	2.433	25.272	0.21
Phon 5	15.49	59.251	2.412	24.565	2.406	24.626	0.25

^a Diff% corresponds to $(V_0 \text{ (relax)} - V_0 \text{ (comp)}) \times 100 / V_0 \text{ (relax)}$.

ρ_{comp} : densities of compacted glasses.

ρ_{relax} : relaxed glass densities measured after first thermal expansion measurements up to T_{13} (temperature at which the viscosity is 10^{13} Pa.s).

Table 4. Experimental length (L in mm) of super-cooled liquids as a function of temperature.

T (K)	L(mm)	T (K)	L(mm)	T(K)	L(mm)	T(K)	L(mm)
<u>Anhy. Albite</u>		<u>Albite-1.3</u>		<u>Albite-2.2</u>			
995.6	4.7421	715.5	6.2238	650.3	4.2749		
1005.5	4.7429	725.5	6.2251	660.4	4.2759		
1015.6	4.7436	725.5	6.2250	670.4	4.2769		
1015.6	4.7438	735.5	6.2263	670.5	4.2770		
1025.6	4.7447	745.5	6.2275	680.4	4.2778		
1035.6	4.7455	755.5	6.2286	690.2	4.2788		
1035.7	4.7455						
1045.6	4.7464						
<u>Anhy. Tephrite</u>		<u>Teph 0.3</u>		<u>Teph 1.5</u>		<u>Teph 3</u>	
880.3	8.8040	820.1	6.8025	750.3	4.9377	680.3	4.6249
890.4	8.8061	820.2	6.8024	760.4	4.9388	690.4	4.6259
890.3	8.8057	830.1	6.8041	770.4	4.9402	700.5	4.6269
900.4	8.8081	840.2	6.8058	780.3	4.9412	700.5	4.6272
900.4	8.8078	840.2	6.8056	790.3	4.9426	710.5	4.6283
900.5	8.8080	850.1	6.8076	800.3	4.9438	720.4	4.6291
910.6	8.8102	850.2	6.8075			720.5	4.6294
910.6	8.8101	860.1	6.8092			730.5	4.6305
920.8	8.8124	860.2	6.8091			740.5	4.6316
<u>Anhy. Trachyte</u>		<u>Trach 1.5</u>		<u>Trach 3.5</u>			
916.1	9.8768	730.4	4.2140	650.5	9.1137		
926.1	9.8792	740.3	4.2153	660.5	9.1162		
936.0	9.8815	740.3	4.2149	670.5	9.1185		
936.2	9.8809	750.4	4.2163	680.5	9.1211		
946.1	9.8838	760.3	4.2173	690.5	9.1238		
946.1	9.8832	770.1	4.2185				
956.1	9.8857						
956.1	9.8862						
966.1	9.8887						
966.1	9.8882						
<u>Anhy. Foidite</u>		<u>NIQ 1.2</u>		<u>NIQ 2.3</u>			
850.3	12.8889	760.3	4.0331	680.5	4.5551		
860.2	12.8919	770.1	4.0340	690.5	4.5563		
870.2	12.8947	780.3	4.0350	700.4	4.5574		
880.4	12.8980	800.2	4.0369	700.5	4.5572		
890.1	12.9009			710.4	4.5586		
900.3	12.9038			710.4	4.5583		
				720.3	4.5595		

Table 5. Thermal expansion of the liquids and glasses (compacted and relaxed ones) and temperature intervals of the thermal expansion of liquids.

Sample	H ₂ O mol%	α_{glass}^* (10 ⁻⁵ K ⁻¹)	$\alpha_{\text{glass}}^{**}$ (10 ⁻⁵ K ⁻¹)	Diff. %	α_{liquid} (10 ⁻⁵ K ⁻¹)	ΔT (K)
Albite						
Alb 0.	0.		1.594		5.418	990 - 1050
Albite-1.3	3.78	2.036	1.937	+ 5%	5.900	715 - 755
Albite-2.2	6.47	2.109	2.006	+ 5%	6.701	650 - 690
Tephrite						
Teph 0.	0.		2.242		7.100	880 - 920
Teph 0.3	1.74	2.317	2.376	- 2%	7.220	820 - 860
Teph 1.5	5.22	2.602	2.455	+ 6%	7.424	750 - 800
Teph 3	8.31	2.525	2.467	+ 2%	7.271	670 - 740
Trachyte						
Trach 0.	0.		2.542		7.055	915 - 965
Trach 1.5	5.42	2.335	2.230	+ 5%	7.859	730 - 770
Trach 3.5	10.12	2.505	2.371	+ 7%	8.296	650 - 690
Foidite***						
NIQ 0.	0.		2.422		6.946	850 - 900
NIQ 1.2	4.03		2.690		7.064	760 - 800
NIQ 2.3	6.83		2.897		7.212	680 - 720

*Thermal expansion coefficient of compacted glasses as synthesized (*cf.* Table 2).

**Thermal expansion coefficient of relaxed glasses.

***Only thermal expansion experiments on relaxed glasses were performed.

Diff.% corresponds to $(\alpha_{\text{glass}}^* - \alpha_{\text{glass}}^{**}) / \alpha_{\text{glass}}^*$.

Table 6. Comparison between measured and calculated hydrous liquid volumes (cm³/mol).

Sample	<i>T</i> (K)	<i>V</i> _{exp}	<i>V</i> _{cal} (1) ^a O-L (99)	^b Diff%	<i>V</i> _{cal} (2) ^a This work	^b Diff%
Albite						
Anhydrous	1030	27.90±0.20	27.72	0.65		
Albite	1040	27.91±0.20	27.73	0.65		
	1050	27.93±0.20	27.74	0.69		
	1060	27.95±0.20	27.75	0.73		
	1070	27.96±0.20	27.76	0.73		
	1080	27.98±0.20	27.77	0.76		
Albite-1.3	780	27.05±0.19	27.13	-0.28	27.11	-0.21
	790	27.06±0.19	27.14	-0.27	27.12	-0.20
	800	27.08±0.19	27.15	-0.26	27.14	-0.20
	810	27.10±0.19	27.17	-0.25	27.15	-0.20
	820	27.11±0.19	27.18	-0.24	27.10	-0.20
	830	27.13±0.19	27.19	-0.22	27.18	-0.19
Albite-2.2	710	26.56±0.19	26.77	-0.78	26.70	-0.55
	720	26.58±0.19	26.78	-0.78	26.72	-0.56
	730	26.59±0.19	26.80	-0.77	26.74	-0.56
	740	26.61±0.19	26.81	-0.76	26.76	-0.56
	750	26.63±0.19	26.83	-0.74	26.78	-0.57
	760	26.65±0.19	26.84	-0.73	26.80	-0.57
Tephrite						
Anhydrous	930	23.29±0.16	23.06	0.97		
Tephrite	940	23.30±0.16	23.08	0.93		
	950	23.32±0.16	23.10	0.94		
	960	23.33±0.16	23.12	0.92		
	970	23.35±0.17	23.14	0.91		
	980	23.37±0.17	23.16	0.92		
Teph 0.3	880	22.99±0.16	22.91	0.37	22.91	0.36
	890	23.01±0.16	22.93	0.35	22.93	0.34
	900	23.02±0.16	22.95	0.34	22.95	0.32
	910	23.05±0.16	22.97	0.33	22.97	0.31
	920	23.06±0.16	22.99	0.31	22.99	0.29
	930	23.08±0.16	23.01	0.30	23.01	0.27
Teph 1.5	810	22.50±0.16	22.62	-0.54	22.61	-0.46
	820	22.52±0.16	22.65	-0.56	22.63	-0.50
	830	22.54±0.16	22.67	-0.59	22.66	-0.54
	840	22.55±0.16	22.69	-0.61	22.68	-0.58
	850	22.57±0.16	22.71	-0.63	22.71	-0.61
	860	22.59±0.16	22.74	-0.66	22.73	-0.65
Teph 3	750	22.13±0.15	22.34	-0.95	22.28	-0.69
	760	22.14±0.16	22.36	-1.00	22.31	-0.75
	770	22.16±0.16	22.39	-1.04	22.34	-0.82
	780	22.17±0.16	22.41	-1.07	22.37	-0.87
	790	22.19±0.16	22.44	-1.11	22.40	-0.93
	800	22.21±0.16	22.46	-1.15	22.43	-1.00
Trachyte						
Anhydrous	970	26.64±0.19	26.30	1.28		
Trachyte	980	26.66±0.19	26.31	1.31		
	990	26.68±0.19	26.33	1.31		
	1000	26.70±0.19	26.34	1.35		
	1010	26.72±0.19	26.35	1.38		

	1020	26.74±0.19	26.36	1.42		
Trach 1.5	760	25.47±0.18	25.62	-0.58	25.58	-0.44
	770	25.49±0.18	25.64	-0.57	25.60	-0.44
	780	25.51±0.18	25.65	-0.55	25.62	-0.44
	790	25.53±0.18	25.67	-0.54	25.64	-0.44
	800	25.55±0.18	25.69	-0.53	25.66	-0.44
	810	25.57±0.18	25.70	-0.51	25.68	-0.44
Trach 3.5	680	24.80±0.17	25.08	-1.13	24.79	-0.65
	690	24.82±0.17	25.10	-1.12	24.81	-0.67
	700	24.84±0.18	25.12	-1.12	25.01	-0.70
	710	24.86±0.18	25.14	-1.12	25.04	-0.72
	720	24.88±0.18	25.16	-1.12	25.06	-0.75
	730	24.90±0.18	25.18	-1.12	25.09	-0.77
Foidite*						
Anhydrous	920	21.54±0.15	21.10	2.04	21.57	-0.13
Foidite	930	21.55±0.15	21.12	1.99	21.59	-0.17
	940	21.57±0.15	21.14	1.98	21.61	-0.17
	950	21.58±0.15	21.16	1.93	21.63	-0.22
	960	21.60±0.15	21.18	1.92	21.65	-0.22
	970	21.61±0.15	21.21	1.87	21.67	-0.26
NIQ 1.2	800	21.03±0.15	20.75	1.33	21.15	-0.57
	810	21.05±0.15	20.78	1.29	21.18	-0.60
	820	21.06±0.15	20.80	1.25	21.20	-0.67
	830	21.08±0.15	20.82	1.20	21.23	-0.70
	840	21.09±0.15	20.85	1.16	21.25	-0.77
	850	21.11±0.15	20.87	1.11	21.28	-0.80
NIQ 2.3	750	20.78±0.15	20.55	1.12	20.87	-0.44
	760	20.80±0.15	20.57	1.07	20.90	-0.48
	770	20.81±0.15	20.60	1.01	20.93	-0.57
	780	20.83±0.15	20.63	0.96	20.96	-0.62
	790	20.84±0.15	20.65	0.91	20.99	-0.71
	800	20.86±0.15	20.68	0.85	21.02	-0.76
Phonolite						
Anhydrous	920	27.62±0.19	27.37	0.90		
Phonolite	930	27.65±0.19	27.39	0.95		
	940	27.67±0.19	27.40	0.96		
	950	27.69±0.19	27.42	0.98		
	960	27.71±0.19	27.44	0.99		
	970	27.73±0.19	27.45	1.00		
Phon 0.8	850	26.92±0.19	26.99	-0.27	26.99	-0.26
	860	26.94±0.19	27.01	-0.25	26.01	-0.25
	870	26.97±0.19	27.03	-0.23	27.03	-0.24
	880	26.99±0.19	27.05	-0.22	27.05	-0.23
	890	27.01±0.19	27.07	-0.20	27.07	-0.22
	900	27.03±0.19	27.08	-0.19	27.09	-0.21
Phon 1.6	730	26.35±0.18	26.51	-0.61	26.47	-0.43
	740	26.38±0.19	26.53	-0.60	26.49	-0.43
	750	26.40±0.19	26.56	-0.58	26.51	-0.43
	760	26.43±0.19	26.58	-0.56	26.54	-0.42
	770	26.45±0.19	26.60	-0.55	26.56	-0.42
	780	26.48±0.19	26.62	-0.53	26.59	-0.42
Phon 3.2	620	25.53±0.18	25.75	-0.89	25.60	-0.23
	630	25.55±0.18	25.78	-0.88	25.62	-0.24
	640	25.58±0.18	25.80	-0.86	25.65	-0.26
	650	25.61±0.18	25.83	-0.85	25.68	-0.27

660	25.64±0.18	25.85	-0.84	25.72	-0.29
670	25.66±0.18	25.88	-0.83	25.74	-0.30

^a V_{cal} (1) is calculated using the model of Lange (1997) and Ochs and Lange (1999). V_{cal} (2) is calculated using the model of Lange (1997) and our new values for $\bar{V}_{\text{H}_2\text{O}}$ and $\frac{d\bar{V}_{\text{H}_2\text{O}}}{dT}$. For the foidite serie V_{cal} (2) is calculated using the following equation:

$$V_{\text{liquid}}(T) = \sum X_i \times \left[\bar{V}_i(T_{\text{ref}}) + \frac{d\bar{V}_i}{dT} \times (T - T_{\text{ref}}) \right] + X_{\text{SiO}_2} X_{\text{CaO}} \left[\bar{V}_{\text{SiO}_2-\text{CaO}}(T_{\text{ref}}) + \frac{d\bar{V}_{\text{SiO}_2-\text{CaO}}}{dT} \times (T - T_{\text{ref}}) \right]$$

^b Diff% corresponds to $(V_{\text{exp}} - V_{\text{cal}}) \times 100 / V_{\text{exp}}$.

Table 7. Parameters of the liquid volume equation (9)

Oxide	\bar{V}_i (cm ³ /mol)	$d\bar{V}_i / dT$ (cm ³ /mol K)	Reference
$T_{\text{ref}} = 1073$ K			
SiO ₂	26.86	0.	Lange (1997)
Al ₂ O ₃	37.42	0.	Lange (1997)
MgO	9.57	$3.27 \cdot 10^{-3}$	Lange (1997)
CaO	14.10	$3.74 \cdot 10^{-3}$	Lange (1997)
Na ₂ O	23.88	$7.68 \cdot 10^{-3}$	Lange (1997)
K ₂ O	38.22	$12.08 \cdot 10^{-3}$	Lange (1997)
TiO ₂ *	28.32	0.	Lange and Carmichael (1987)
TiO ₂ *	23.87	0.	Lange and Carmichael (1987)
$T_{\text{ref}} = 1273$ K			
H ₂ O	22.89	$9.55 \cdot 10^{-3}$	Ochs and Lange (1999)
H ₂ O	23.80	$15.85 \cdot 10^{-3}$	This work
$T_{\text{ref}} = 1873$ K			
SiO ₂	27.297	$1.157 \cdot 10^{-3}$	Courtial and Dingwell (1999)
Al ₂ O ₃	36.666	$-1.184 \cdot 10^{-3}$	Courtial and Dingwell (1999)
MgO	12.662	$1.041 \cdot 10^{-3}$	Courtial and Dingwell (1999)
CaO	20.664	$3.756 \cdot 10^{-3}$	Courtial and Dingwell (1999)
SiO ₂ -CaO	-7.105	$-2.138 \cdot 10^{-3}$	Courtial and Dingwell (1999)

*The partial molar volume of TiO₂ is 28.32 cm³/mol and 23.87 cm³/mol in sodium and calcium silicate liquids, respectively (Lange and Carmichael, 1987).

Table 8. Linear fits of the molar volume (cm^3/mol) of glasses and liquids and thermal expansivity of glasses and liquids in the albite, tephrite, trachyte and foidite hydrous compositions.

Sample	α_{glass}	$(dV/dT)_{\text{glass}}$ ($10^{-3} \text{ cm}^3 \text{ mol}^{-1} \text{ K}^{-1}$)	$\Delta T (\text{K})^a$	α_{liquid}	$(dV/dT)_{\text{liquid}}$ ($10^{-3} \text{ cm}^3 \text{ mol}^{-1} \text{ K}^{-1}$)	$\Delta T (\text{K})^a$	$T_{12} (\text{K})^b$
Albite							
Alb 0.	27.444	0.44	300-1000	26.353	1.50	990-1050	1032
Albite-1.3	26.644	0.52	300-700	25.802	1.60	715-755	784
Albite-2.2	26.181	0.53	300-640	25.191	1.79	650-690	712
Tephrite							
Teph 0.	22.806	0.52	300-860	21.754	1.65	880-920	933
Teph 0.3	22.516	0.54	300-810	21.526	1.67	820-860	878
Teph 1.5	22.058	0.55	300-740	21.149	1.67	750-800	814
Teph 3	21.719	0.54	300-660	20.910	1.62	670-740	750
Trachyte							
Trach 0.	25.990	0.67	300-900	24.824	1.87	915-965	970
Trach 1.5	25.041	0.57	300-720	23.951	2.00	730-770	760
Trach 3.5	24.398	0.58	300-640	23.396	2.06	650-690	680
Foidite							
NIQ 0.	21.059	0.52	300-830	20.156	1.50	850-900	916
NIQ 1.2	20.583	0.56	300-740	19.848	1.48	760-800	800
NIQ 2.3	20.333	0.60	300-670	19.656	1.50	680-720	750

^a Temperature interval for the experiments for the glasses and super-cooled liquids.

^b $T_{12} (\text{K})$ is the temperature at which the viscosity is 10^{12} Pa.s .